



HAL
open science

Enlacement and interlacement shape descriptors

Michaël Clément, Camille Kurtz, Laurent Wendling

► **To cite this version:**

Michaël Clément, Camille Kurtz, Laurent Wendling. Enlacement and interlacement shape descriptors. International Conference on Pattern Recognition and Artificial Intelligence (ICPRAI), 2020, Zhongshan, China. hal-02492607

HAL Id: hal-02492607

<https://hal.science/hal-02492607>

Submitted on 27 Feb 2020

HAL is a multi-disciplinary open access archive for the deposit and dissemination of scientific research documents, whether they are published or not. The documents may come from teaching and research institutions in France or abroad, or from public or private research centers.

L'archive ouverte pluridisciplinaire **HAL**, est destinée au dépôt et à la diffusion de documents scientifiques de niveau recherche, publiés ou non, émanant des établissements d'enseignement et de recherche français ou étrangers, des laboratoires publics ou privés.

Enlacement and Interlacement Shape Descriptors

Michaël Clément¹, Camille Kurtz², and Laurent Wendling²

¹ Univ. Bordeaux, CNRS, Bordeaux INP, LaBRI UMR 5800, 33400 Talence, France

² Université de Paris, LIPADE, 75006 Paris, France

Abstract. We propose a novel approach to characterize complex 2D shapes based on enlacement and interlacement directional spatial relations. This new relational concept allows to assess in a polar space how the concave parts of objects are intertwined following a set of directions. In addition, such a spatial relationship has an interesting behavior considering the common properties in pattern recognition such as translation, rotation, scale and symmetry. A shape descriptor is defined by considering the enlacement of its own shape and the disk area that surrounds it. An experimental study carried out on two datasets of binary shapes highlights the discriminating ability of these new shape descriptors.

Keywords: shape descriptors · spatial relations · enlacement · interlacement

1 Introduction

A 2D shape recognition system is usually roughly decomposed into several successive steps [1, 2]. First, the shapes are extracted from their surrounding background. This step, called segmentation, relies heavily on *a priori* knowledge of the images to be processed. Then, a new representation is built from the extracted patterns. This representation aims to computationally judge the similarity or distance between two patterns, usually to perform classification. It may either be a set of measurements made on the patterns, forming a vector of features, or a symbolic description of how the pattern can be divided into basic shapes. The choice of one representation instead of another one generally relies on the application under consideration, and following underlying conditions such as robustness against noise and small distortions, invariance with regards to common geometrical transformations or tolerance to occlusions. The shape representation for object recognition has been the subject of numerous researches; and extensive surveys of shape analysis can be found in the literature, for example in [3–5]. Two main categories of shape descriptors are often encountered: those working on a shape as a whole (called region-based descriptors) and those working on the contours of the shape (called contour-based descriptors).

The usual descriptors based on the contours include the well-known Fourier descriptors [6–8] and the curvature approaches [9, 10], where a shape is described in a scale space. The shape context [11] is also a robust descriptor to small perturbations of parts of the shape. The main drawback lies in the lack of guarantee with scale-invariance. Other approaches are based on the extraction of the

skeleton considering [12, 13] (for instance, a graph defined from the medial axis). Shock graphs associated to both global optimization and graph matching provide a powerful tool [14] for discriminating shapes but such methods are generally highly sensitive to scale variations. Since contour descriptors are based on the boundary of a shape, they are not able to properly capture the internal structure of a shape. Furthermore, such methods are not suitable for disjoint shapes or shapes with holes because boundary information is not available. Therefore, they remain limited to certain types of applications.

Region-based descriptors work on a shape as a whole taking into account all the pixels within it. Comparative studies [15, 16] have demonstrated the interest of the Zernike moments, and numerous researches have been focused on improving their invariance properties [17] and speeding up the fast computation of the Zernike moments [18]. Fourier-Mellin has been introduced to avoid the mathematical application problems of the standard transform but an approximation is required to process with numerical data [19]. To overcome the drawbacks of contour based Fourier descriptors, Zhang and Lu [8] have proposed a region-based generic Fourier descriptor based on the polar discrete transform. Experimental results show that this approach outperforms common contour-based (classical Fourier and curvature approaches) and region-based (Zernike moments) shape descriptors. These methods were often adapted to deal with the specificities of the application under consideration. On the whole, region-based methods are more suited to general applications. However, they are generally more computationally intense and most approaches need to normalize (centroid position, re-sampling) the image to be processed with geometrical properties. Such a normalization may introduce errors, sensitivity to noise, and consequently inaccuracy in the recognition / decision process.

Among region-based descriptors, relative position descriptors aim at assessing a specific measure following a set of directions. Most of the works have been focused on the notions on force histogram [20], phi-descriptor [21], meta directional histogram [22] built from fuzzy landscapes [23] and Radon transform [24]. Such methods are less sensitive to the noise and they preserve common geometrical properties. They are generally less relevant when the number of classes grows drastically due to the compact aspect of the descriptor but they offer important (complementary) information when they are combined with other descriptors.

In this paper, our contribution is the proposition of a novel region-based approach in the context of this generic shape recognition problem. The underlying strategy of our method is to capture how the parts of one object are messed or twisted from a circular background area, enabling capture more complex patterns, whose shapes are, for instance, affected by complex concavities and (deep) levels of imbrication. The remainder of this article is organized as follows. Section 2 recalls the concept of directional spatial enlacement, initially proposed in [25]. From this model, we derive novel shape descriptors, presented in Section 3 and Section 4, which are defined by considering the enlacement / interlacement of the object shape and the disk area surrounding it. An experimental

study carried out on two databases of binary shapes is described in Section 5. Finally, conclusions and perspectives will be found in Section 6.

2 Directional Spatial Enlacement

The notion of directional spatial enlacement, modeled as an “enlacement” histogram, was initially proposed to assess a new spatial relation between two binary objects [25]. Such a histogram was also embedded in pattern recognition applications considering local features calculated from pairs of broad objects [26]. We show here that it can be easily used to provide a discriminate descriptor (or signature) characterizing only one shape. We recall first basic notions aiming at describing such a kind of signature that efficiently integrates both whole shape and spatial description following a set of directions. A full description of the underlying theoretical developments can be found in [27, 25].

Let (A, B) be a couple of two-dimensional objects. The goal is to measure how an object A is enlaced with an object B (and reciprocally).

Handling with points The relative positions of individual points $a_i \in A$ and $b_i \in B$ are considered as arguments to put in favor of the proposition “ A is enlaced by B ”. Let us consider an oriented straight line $\Delta^{(\theta, \rho)}$. The functions $f_A^{(\theta, \rho)}$ and $f_B^{(\theta, \rho)}$ designate longitudinal cuts along the oriented line $\Delta^{(\theta, \rho)}$. The quantity of A located *after* a point x on a line $\Delta^{(\theta, \rho)}$ is given by:

$$\int_x^{+\infty} f_A^{(\theta, \rho)}(y) dy. \quad (1)$$

Handling with segments Let us consider a binary object A . The integral determines the cumulated length of the segments on the interval $[x, +\infty[$ of this longitudinal cut. Consequently, to capture the quantity of A located *after* points of B on this line, we have:

$$\int_{-\infty}^{+\infty} f_B^{(\theta, \rho)}(x) \int_x^{+\infty} f_A^{(\theta, \rho)}(y) dy dx. \quad (2)$$

Symmetrically, the quantity of A located *before* parts of B is obtained with:

$$\int_{-\infty}^{+\infty} f_A^{(\theta, \rho)}(x) \int_x^{+\infty} f_B^{(\theta, \rho)}(y) dy dx. \quad (3)$$

The goal is then to combine these two quantities, in order to take into account both parts of B *before* and *after* parts of A , leading us to the following general definition of the one-dimensional enlacement. Let f and g be two bounded measurable functions with compact support from \mathbb{R} to \mathbb{R} . The enlacement of f with regards to g is defined as:

$$E(f, g) = \int_{-\infty}^{+\infty} g(x) \int_x^{+\infty} f(y) \int_y^{+\infty} g(z) dz dy dx. \quad (4)$$

This generic definition between two real-valued functions can be applied to longitudinal cuts $f_A^{(\theta,\rho)}$ and $f_B^{(\theta,\rho)}$. The value $E(f_A^{(\theta,\rho)}, f_B^{(\theta,\rho)})$ represents the overall enlacement of A by B along the oriented line $\Delta^{(\theta,\rho)}$.

Handling with objects Let $\theta \in \mathbb{R}$ be an orientation angle and let us consider the pencil of all parallel lines $\{\Delta^{(\theta,\rho)}, \rho \in \mathbb{R}\}$ in this direction; they will slice any object into a pencil of longitudinal cuts. The enlacement of an object with regards to another in this direction θ , is obtained by aggregating all the one-dimensional enlacement values, as it follows. Let $\theta \in \mathbb{R}$ be an orientation angle, and let A and B be two objects. The enlacement of A by B in the direction θ is given by:

$$E_{AB}(\theta) = \int_{-\infty}^{+\infty} E(f_A^{(\theta,\rho)}, f_B^{(\theta,\rho)}) d\rho. \quad (5)$$

Properties Considering the definition of the enlacement from parallel longitudinal cuts, the following properties can be easily checked [25]:

- For any two objects A and B , the directional enlacement E_{AB} is **periodic** with period π , that is $\forall \theta \in \mathbb{R}, E_{AB}(\theta) = E_{AB}(\theta + k\pi), k \in \mathbb{Z}$;
- For any two objects A and B , the directional enlacement E_{AB} is invariant with regards to **translations**. Let T_v by a translation by a vector $v \in \mathbb{C} \simeq \mathbb{R}^2$, we have: $E_{T_v(A)T_v(B)}(\theta) = E_{AB}(\theta)$;
- For any two objects A and B , the directional enlacement E_{AB} is quasi-invariant with regards to **rotations**. Let $\alpha \in \mathbb{R}$ be a rotation angle and let R_α be a rotation transformation, we have: $E_{R_\alpha(A)R_\alpha(B)}(\theta) = E_{AB}(\theta - \alpha)$;
- For any two objects A and B , the directional enlacement E_{AB} is quasi-invariant with regards to **scaling** transformations. Let $\lambda \in \mathbb{R}$ be a scaling factor and let S_λ be a scaling transformation, we have: $E_{S_\lambda(A)S_\lambda(B)}(\theta) = \lambda^4 E_{AB}(\theta)$.

3 Enlacement Descriptor

In its initial definition, the enlacement is calculated between two generic binary objects A and B . Considering one single shape, a longitudinal cut can split it into several segments assuming the existence of holes or concavities. The goal is to assess such internal information by calculating the enlacement between a shape and a surrounding area (including the convex hull). Let us consider a shape A and its centroid $c_A(x_a, y_a)$. Let r_A be the maximal radius of A , calculated from c_A . The surrounding area, noted \bar{A} is defined from the disk D of center c_A and radius r_A such that: $\bar{A} = D \setminus A$ (that is $D = A \cup \bar{A}$).

The scalar enlacement value in a given direction should be relative to the overall area in order to compare the enlacement of different couples of shapes having the same area (but different shapes). Let us define the area $\|A\|_1$ of a shape A by:

$$\|A\|_1 = \iint_{\mathbb{R}^2} |f_A(x, y)| dx dy. \quad (6)$$

The directional enlacement descriptor of A with regards to \bar{A} is defined by the following function (with $\mathcal{E}_{A\bar{A}}$ is equal to 0 if $A = D$):

$$\begin{aligned} \mathcal{E}_{A\bar{A}} : \mathbb{R} &\longrightarrow \mathbb{R} \\ \theta &\longmapsto \frac{E_{A\bar{A}}(\theta)}{\|A\|_1 (\pi r_{\bar{A}}^2 - \|A\|_1)}. \end{aligned} \quad (7)$$

The enlacement descriptor $\mathcal{E}_{A\bar{A}}$ takes the form of a function, which associates to each angle θ the enlacement value of A by its surrounding area \bar{A} normalized by the combination of the two respective areas. Note that both descriptors $\mathcal{E}_{A\bar{A}}$ and $\mathcal{E}_{\bar{A}A}$ provide complementary information (*i.e.* enlacement of the enclosing circle by the shape, and enlacement of the shape by the enclosing circle respectively). In this sense, they can also be concatenated into a single feature vector $\mathcal{E}_{A\bar{A}} \mathcal{E}_{\bar{A}A}$.

An overall number of elementary occurrences of enlacement is obtained by considering each longitudinal cut of the shape in direction θ . The descriptor can be interpreted as a circular histogram, which we call the \mathcal{E} -*histogram*. Using a disk area as an overlapping support instead of a rectangle area keeps consistency (in an isotropic manner), considering the pencil of longitudinal cuts following any direction, as the same amount of pairwise information is processed. Thanks to this normalization the enlacement histogram $\mathcal{E}_{A\bar{A}}$ is invariant with regards to scaling transformations, that is: let $\lambda \in \mathbb{R}$ be a scaling factor and let S_λ be the associated scaling transformation; we have: $\mathcal{E}_{S_\lambda(A)S_\lambda(\bar{A})}(\theta) = \mathcal{E}_{A\bar{A}}(\theta)$.

It is easy to show that the properties of periodicity (considering opposite directions), translation (as shapes are processed independently of their location in the frame) and rotation (a rotation of angle θ implies a circular shift of θ in the descriptor) are preserved from $E_{A\bar{A}}$ for the enlacement histogram $\mathcal{E}_{A\bar{A}}$. Then \mathcal{E} -histogram of a shape is invariant with regards to translations and scaling transformations, and quasi-invariant to rotations.

4 Interlacement Descriptor

The enlacement histogram $\mathcal{E}_{A\bar{A}}$ defines a shape descriptor that quantitatively characterizes how a shape A is enlaced by its surrounding background \bar{A} . As a relative position descriptor, the descriptor $\mathcal{E}_{A\bar{A}}$ does not completely describe the spatial configuration of A and \bar{A} . So the opposite descriptor $\mathcal{E}_{\bar{A}A}$ is complementary to $\mathcal{E}_{A\bar{A}}$ and can also be considered to improve the description of the shape under consideration. The combination of these two descriptors provides a description of the mutual interlacement of the shape and its surrounding area. The directional interlacement descriptor is defined by the harmonic mean as:

$$\mathcal{I}_{A\bar{A}}(\theta) = \frac{2 \mathcal{E}_{A\bar{A}}(\theta) \times \mathcal{E}_{\bar{A}A}(\theta)}{\mathcal{E}_{A\bar{A}}(\theta) + \mathcal{E}_{\bar{A}A}(\theta)} \quad (8)$$

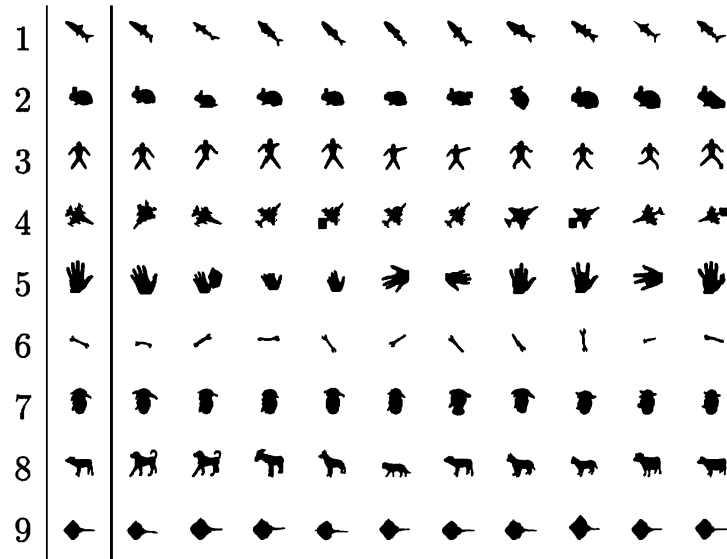


Fig. 1. Binary 2D shapes from the Sharvit B_1 dataset (99 shapes, 9 classes). Similarly, the Sharvit B_2 contains 216 shapes (12 classes) with the same kind of distortions.

The interlacement descriptor can also be interpreted as a circular histogram, called the \mathcal{I} -*histogram*. The invariance properties are preserved for the interlacement histogram.

5 Experimental study

For this experimental study, the proposed descriptors have been employed for a 2D shape classification task on two datasets of binary shapes followed by a comparative study involving other baseline shape descriptors.

5.1 Datasets

Two shape datasets have been considered to highlight the interest of our proposed enlacement and interlacement shape descriptors.

Sharvit B_1 and B_2 The first shape dataset is provided by Sharvit *et al.* [28]. This dataset is decomposed into two independent datasets, B_1 that contains 9 categories with 11 binary shapes in each category (see Figure 1) and B_2 that contains 18 categories with 12 shapes in each category. Considering B_1 , a few of the shapes are occluded (airplanes and hands) and some shapes are partially represented (rabbits, men, and hands). There are also distorted objects (tools)

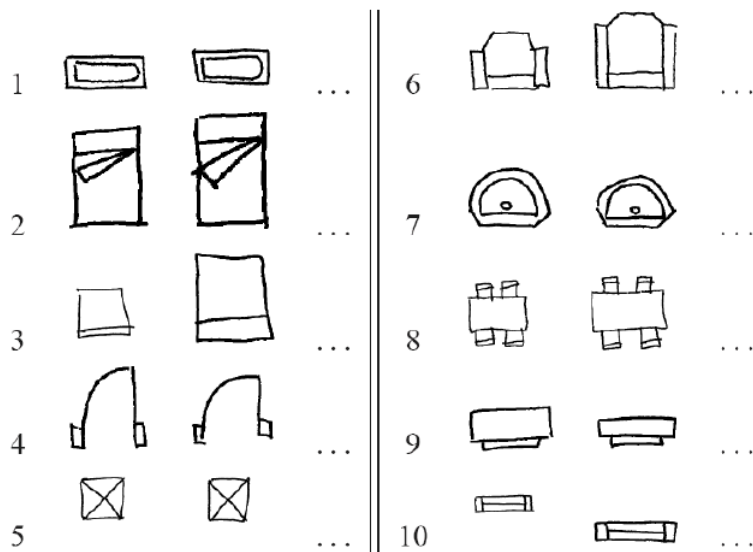


Fig. 2. Samples from the CVC dataset composed of 3000 binary 2D shapes (300 classes) representing various hand-drawn patterns.

and heterogeneous shapes in the same cluster (animals). The dataset B_2 also contains shapes with similar distortions. These two Sharvit sub-datasets are widely used in the literature to compare feature descriptors designed to classify 2D shapes in presence of noise, artifacts and distorted parts.

CVC The second dataset consists of 3000 binary shapes categorized into 10 classes, with equal number of samples in each category (see Figure 2). It is kindly provided by CVC Barcelona. This dataset is composed of complex 2D hand-drawn patterns, with shapes having holes and disconnected parts. The patterns were drawn by ten persons using the Anoto digital pen and paper.

5.2 Experimental protocol

We used the proposed enlacement and interlacement descriptors to classify the binary shapes from the Sharvit and CVC datasets into their corresponding categories. For the first experiment, we studied the influence of the number of directions for our proposed descriptors (as well as their potential combinations) on the Sharvit dataset, since this baseline dataset contains more generic and heterogeneous shapes. Then, we evaluated the impact of using different classifiers on the larger CVC dataset. For both datasets, we also perform a comparative study with other baseline shape descriptors.

Parameter settings For each 2D shape of the datasets, we computed both enlacement shape descriptors $\mathcal{E}_{A\bar{A}}$ and $\mathcal{E}_{\bar{A}A}$, as well as the interlacement descriptor \mathcal{I}_A . All these descriptors are computed onto a set of k discrete directions (the influence of k being studied hereinafter) equally spaced along the $[0, \pi]$ interval.

The resulting feature vectors are used to train different classifiers to recognize the different shape categories from the two datasets. In these experiments, we tested:

- k -nearest neighbors classifiers (k -NN) using the ℓ_2 norm on features. The number of neighbors has been empirically set to $k = 1$ (for both datasets, using more neighbors did not improve the results, either for majority of weighted votes);
- SVM classifiers following a *one-versus-all* strategy for multiclass classification. The soft-margin hyperparameter C was optimized by performing grid search on the training set for each tested features. We report results for SVMs using linear and gaussian kernels.

To better assess the robustness of the approach, this classification process is coupled with a cross validation strategy. For both the Sharvit B_1 and B_2 datasets, we employed a leave-one-out strategy, as these datasets are relatively small. For the CVC dataset we used a k -fold cross validation strategy with $k = 3$. That is, the training set representing 2/3 of its total size, while the remaining 1/3 is used for testing, and this process is repeated 3 times so that the whole dataset is classified. For each strategy, we evaluate the classification results using the accuracy score (*i.e.* the rate of correctly classified shapes).

5.3 Influence of the number of directions

In this first experiment, we studied the influence of the number of discrete directions $k \in [0, \pi]$ when computing the enlacement descriptors $\mathcal{E}_{A\bar{A}}$ and $\mathcal{E}_{\bar{A}A}$, the interlacement \mathcal{I}_A , as well as their combinations $\mathcal{E}_{A\bar{A}} \mathcal{E}_{\bar{A}A}$ and $\mathcal{E}_{A\bar{A}} \mathcal{E}_{\bar{A}A} \mathcal{I}_A$. Note that when combining descriptors, the size is increased accordingly: $\mathcal{E}_{A\bar{A}} \mathcal{E}_{\bar{A}A}$ has $2k$ values and $\mathcal{E}_{A\bar{A}} \mathcal{E}_{\bar{A}A} \mathcal{I}_A$ has $3k$ values. The different numbers of directions tested were $k \in \{4, 8, 16, 32, 64\}$. For all of these values, we apply the k -NN classifier with the corresponding descriptors on both Sharvit datasets B_1 and B_2 , following the leave-one-out cross validation strategy.

Figure 3 presents the evolution of the accuracy scores for these different number of directions, on Sharvit (a) B_1 and (b) B_2 . On B_1 , we can observe relatively stable recognition rates for small number of directions, with a slight decrease in performance when using 64 directions. The instability is probably due to the small size of this dataset. For B_2 , we observe a more homogeneous increase in accuracy for all features when increasing the number directions, reaching a plateau for 16-32 directions. Overall, experiments with 32 directions seem to be a good compromise between performance and size. This value will therefore be retained for the remainder of the experimental study.

From these results, we can also observe the relative performances of the different considered features. In particular, we can see that the combination $\mathcal{E}_{A\bar{A}} \mathcal{E}_{\bar{A}A}$

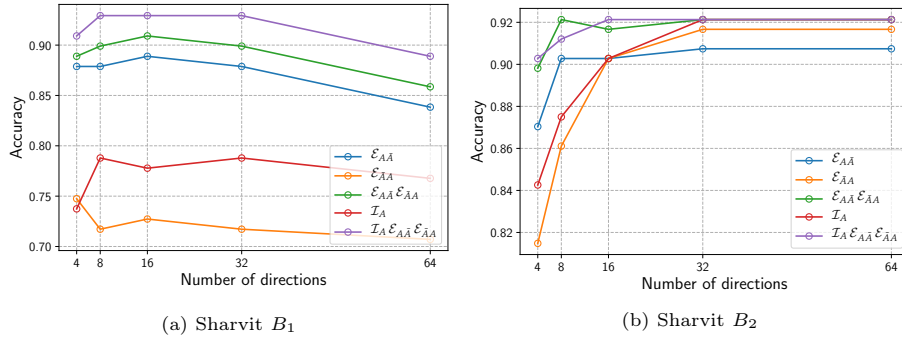


Fig. 3. Accuracy scores for the Sharvit B_1 and B_2 datasets, for varying number of directions of the enlacement and interlacement shape descriptors. Classification is performed with k -NN ($k = 1$) on the ℓ_2 -norm and using leave-one-out cross validation.

of both enlacement descriptors seems to always improve the results compared to their individual parts. Further combining into $\mathcal{E}_{AA} \mathcal{E}_{AA} \mathcal{T}_A$ again slightly improves performance. This seems to confirm our hypothesis that these descriptors represent complementary rich information, captured both from the shape itself and its background counterpart, that can be useful to better characterize complex visual patterns.

5.4 Comparative study and discussion

We now present a comparative study with several commonly used shape descriptors from the literature on both datasets. In these experiments, we used the following baseline descriptors:

- Angular Signature (AS) [29];
- Yang [30];
- 7 Moments of Zernike (Zernike7) [18];
- Angular Radial Transform (ART) [31];
- Generic Fourier Descriptors (GFD) [8];
- Force Histograms (\mathcal{F}_0^{AA} and \mathcal{F}_2^{AA}) [20].

All these methods result in feature vectors for each shape, and are supposed to be relatively robust to different affine transforms such as translation, rotation, or scaling. The five first methods are global shape descriptors, while Force Histograms are based on spatial relations concepts, similarly to our proposed approach. For each of these methods, we use the same experimental protocol defined earlier: leave-one-out for Sharvit (with k -NN), and 3-fold cross validation for CVC (with k -NN and SVMs).

In Table 1, we report the accuracy scores obtained on the Sharvit B_1 and B_2 datasets for the five baseline methods, and we compare them to our proposed enlacement and interlacement descriptors, as well as their combinations.

Table 1. Accuracy scores obtained on the Sharvit datasets B_1 and B_2 with a 1-NN classification (leave-one-out). On the left are the results for the baseline descriptors. On the right are the results for our proposed enlacement and interlacement descriptors, as well as their combinations. Best and second best scores are respectively depicted in bold and underlined.

Baseline descriptors	B_1	B_2	Our descriptors	B_1	B_2
AS	75.76	67.59	$\mathcal{E}_{A\bar{A}}$	87.88	90.74
Yang	82.83	81.94	$\mathcal{E}_{\bar{A}A}$	71.72	<u>91.67</u>
Zernike7	<u>93.94</u>	92.59	\mathcal{I}_A	78.79	92.13
ART	<u>93.94</u>	94.44	$\mathcal{E}_{A\bar{A}} \mathcal{E}_{\bar{A}A}$	<u>89.90</u>	92.13
GFD	95.96	<u>93.06</u>	$\mathcal{I}_A \mathcal{E}_{A\bar{A}} \mathcal{E}_{\bar{A}A}$	92.93	92.13
\mathcal{F}_0^{AA}	77.78	74.54			
\mathcal{F}_2^{AA}	56.57	51.85			

From this Table, we can observe that our proposed shape descriptors provide competitive and comparable results with the tested baseline descriptors. On this dataset, the best accuracy scores were achieved using global descriptors such as GFD, ART or Zernike moments, which can be considered as relevant baselines. Our descriptors that combine pairwise enlacements and also interlacement outperform common directional based descriptors (*i.e.* Force Histograms \mathcal{F}_0^{AA} and \mathcal{F}_2^{AA}). Although some shapes present concavities, most of the them are relatively compact, which can be crippling for our enlacement criterion.

In Table 2 we report the accuracy scores obtained on the larger CVC dataset for the GFD baseline descriptors, and we compare them to our proposed enlacement and interlacement descriptors. Here, we also report results for different classifiers, *i.e.* k -NN and SVMs with linear and gaussian kernels. On this dataset, our combined enlacement and interlacement features significantly improve upon GFD descriptors (with 36 bins as suggested by [8]). We also found that increasing the number of bins for the GFD descriptors to 96 values (*i.e.* to match the dimensionality of our combined features) results in slightly worse performance (from 0.7% to 4% lower accuracy scores depending on the classifier).

Table 2. Accuracy scores obtained on the CVC dataset with different classifiers (k -NN and SVMs with linear and gaussian kernels), following a 3-fold cross validation. Best and second best scores are respectively depicted in bold and underlined.

	k -NN ($k = 1$)	SVM (linear)	SVM (gaussian)
GFD	89.57	87.83	90.43
$\mathcal{E}_{A\bar{A}}$	83.13	90.17	90.57
$\mathcal{E}_{\bar{A}A}$	83.87	87.43	89.87
\mathcal{I}_A	85.73	88.17	90.23
$\mathcal{E}_{A\bar{A}} \mathcal{E}_{\bar{A}A}$	93.83	96.30	96.87
$\mathcal{I}_A \mathcal{E}_{A\bar{A}} \mathcal{E}_{\bar{A}A}$	94.73	96.53	97.00

The good performance of our method on this dataset can be explained by the fact that the shapes are more complex, usually with multiple line strokes resulting in many concavities. The enlacement is specifically designed to capture the internal structure of this types of shapes, characterizing the alternating patterns between strokes in different directions. Therefore, our proposed features seem to be more efficient and powerful for this type of application.

6 Conclusion

A new shape descriptor based on the assessment of both enlacement and interlacement behavior following a set of directions has been proposed in this paper. Experimental study on three databases attests of the promising interest of such directional descriptors which can easily keep nice properties as homothety, relation and translation. Further works are dedicated to extending our descriptors by considering, for instance, the skeleton and the remaining medial axis calculated between the shape and the surrounding area. The goal will be to provide a suitable derivative approach to make tests on other complex specific datasets (such as symbols, texts) where the underlying structure is close to the skeleton (following the width). We plan also to integrate the Chanfrein distance (as in [32]) to better integrate the internal structure of the shape.

References

1. A.K. Jain, R.P.W. Duin, and J. Mao. Statistical pattern recognition: A review. *IEEE Transactions on Pattern Analysis and Machine Intelligence*, 22(1):4–37, 2000.
2. A.W.M. Smeulders, M. Worring, S. Santini, A. Gupta, and R.C. Jain. Content-based image retrieval at the end of the early years. *IEEE Transactions on Pattern Analysis and Machine Intelligence*, 22(12):1349–1380, 2000.
3. S. Loncaric. A survey of shape analysis techniques. *Pattern Recognition*, 31(8):983–1001, 1998.
4. D. Zhang and G. Lu. Review of shape representation and description techniques. *Pattern Recognition*, 37(1):1–19, 2004.
5. C.H. Chen. *Handbook of Pattern Recognition and Computer Vision*. World Scientific, 5th edition, 2016.
6. H. Kauppinen, T. Seppänen, and M. Pietikäinen. An experimental comparison of autoregressive and fourier-based descriptors in 2d shape classification. *IEEE Transactions on Pattern Analysis and Machine Intelligence*, 17(2):201–207, 1995.
7. E. Persoon and K.S. Fu. Shape discrimination using fourier descriptors. *IEEE Transactions on Pattern Analysis and Machine Intelligence*, 8(3):388–397, 1986.
8. D. Zhang and G. Lu. Shape-based image retrieval using generic fourier descriptor. *Signal Processing: Image Communication*, 17(10):825–848, 2002.
9. F. Mokhtarian and S. Abbasi. Shape similarity retrieval under affine transforms. *Pattern Recognition*, 35(1):31–41, 2002.
10. C. Urdiales, A. Bandera, and F.S. Hernández. Non-parametric planar shape representation based on adaptive curvature functions. *Pattern Recognition*, 35(1):43–53, 2002.

11. S.J. Belongie, J. Malik, and J. Puzicha. Shape matching and object recognition using shape contexts. *IEEE Transactions on Pattern Analysis and Machine Intelligence*, 24(4):509–522, 2002.
12. B.B. Kimia, A.R. Tannenbaum, and S.W. Zucker. Shapes, shocks, and deformations I: the components of two-dimensional shape and the reaction-diffusion space. *International Journal of Computer Vision*, 15(3):189–224, 1995.
13. S.H. Zhu and A.L. Yuille. FORMS: A flexible object recognition and modelling system. *International Journal of Computer Vision*, 20(3):187–212, 1996.
14. K. Siddiqi, A. Shokoufandeh, S.J. Dickinson, and S.W. Zucker. Shock graphs and shape matching. *International Journal of Computer Vision*, 35(1):13–32, 1999.
15. C.H. Teh and R.T. Chin. On image analysis by the methods of moments. *IEEE Transactions on Pattern Analysis and Machine Intelligence*, 10(4):496–513, 1988.
16. R.R. Bailey and M.D. Srinath. Orthogonal moment features for use with parametric and non-parametric classifiers. *IEEE Transactions on Pattern Analysis and Machine Intelligence*, 18(4):389–399, 1996.
17. Y. Bin and P. Jia-Xiong. Invariance analysis of improved zernike moments. *Journal of Optics A: Pure and Applied Optics*, 4(6):606–614, 2002.
18. A. Khotanzad and Y.H. Hong. Invariant image recognition by zernike moments. *IEEE Transactions on Pattern Analysis and Machine Intelligence*, 12(5):489–497, 1990.
19. F. Ghorbel. A complete invariant description for gray-level images by the harmonic analysis approach. *Pattern Recognition Letters*, 15(10):1043–1051, 1994.
20. P. Matsakis and L. Wendling. A new way to represent the relative position between areal objects. *IEEE Transactions on Pattern Analysis and Machine Intelligence*, 21(7):634–643, 1999.
21. P. Matsakis, M. Naeem, and F. Rahbarnia. Introducing the Φ -descriptor - A most versatile relative position descriptor. In *ICPRAM, Proceedings*, pages 87–98, 2015.
22. A. Delaye and E. Anquetil. Learning of fuzzy spatial relations between handwritten patterns. *International Journal of Data Mining, Modelling and Management*, 6(2):127–147, 2014.
23. I. Bloch. Fuzzy relative position between objects in image processing: A morphological approach. *IEEE Transactions on Pattern Analysis and Machine Intelligence*, 21(7):657–664, 1999.
24. S. Tabbone and L. Wendling. Binary shape normalization using the radon transform. In *DGCI, Proceedings*, pages 184–193, 2003.
25. M. Clément, A. Poulénard, C. Kurtz, and L. Wendling. Directional enlacement histograms for the description of complex spatial configurations between objects. *IEEE Transactions on Pattern Analysis and Machine Intelligence*, 39(12):2366–2380, 2017.
26. M. Clément, M. Coustaty, C. Kurtz, and L. Wendling. Local enlacement histograms for historical drop caps style recognition. In *ICDAR, Proceedings*, pages 299–304, 2017.
27. M. Clément, C. Kurtz, and L. Wendling. Fuzzy directional enlacement landscapes. In *DGCI, Proceedings*, pages 171–182, 2017.
28. D. Sharvit, J. Chan, H. Tek, and B.B. Kimia. Symmetry-based indexing of image databases. *Journal of Visual Communication and Image Representation*, 9(4):366–380, 1998.
29. T. Bernier and J.A. Landry. A new method for representing and matching shapes of natural objects. *Pattern Recognition*, 36(8):1711–1723, 2003.

30. S. Yang. Symbol recognition via statistical integration of pixel-level constraint histograms: A new descriptor. *IEEE Transactions on Pattern Analysis and Machine Intelligence*, 27(2):278–281, 2005.
31. W.Y. Kim. A new region-based shape descriptor. *ISO/IEC MPEG99/M5472*, 1999.
32. S. Tabbone, L. Wendling, and J.P. Salmon. A new shape descriptor defined on the radon transform. *Computer Vision and Image Understanding*, 102(1):42–51, 2006.